RATE ACCELERATION OF ATP HYDROLYSIS BY F_1F_0-ATP SYNTHASE

ALAN E. SENIOR*, SASHI NADANACIVA AND JOACHIM WEBER

Department of Biochemistry and Biophysics, University of Rochester Medical Center, Rochester, NY 14642, USA

*e-mail: alan_senior@urmc.rochester.edu

Summary

The rate acceleration of ATP hydrolysis by F_1F_0-ATP synthase is of the order of 10^{11}-fold. We present a cyclic enzyme mechanism for the reaction, relate it to known F_1 X-ray structure and speculate on the linkage between enzyme reaction intermediates and subunit rotation. Next, we describe five factors known to be important in the *Escherichia coli* enzyme for the rate acceleration. First, the provision of substrate binding energy by residues lining the catalytic site is substantial; β-Lys155 and β-Arg182 are specific examples, both of which differentially support substrate MgATP *versus* product MgADP binding. Second, octahedral coordination of the Mg^{2+} in MgATP is crucial for both catalysis and catalytic site asymmetry. The residues involved are β-Thr156, β-Glu185 and β-Asp242. Third, there is stabilization of a pentacoordinate phosphorus catalytic transition state by residues β-Lys155, β-Arg182 and α-Arg376. Fourth, residue β-Glu181 binds the substrate water and stabilizes the catalytic transition state. Fifth, there is strong positive catalytic cooperativity, with binding of MgATP at all three sites yielding the maximum rate (V_{max}); the molecular basis of this factor remains to be elucidated.

Key words: ATP synthesis, F_1F_0-ATP synthase, rate acceleration, enzymatic mechanism, molecular mechanism.

Introduction

F_1F_0-ATP synthase carries out two reactions, ATP synthesis and ATP hydrolysis. The first occurs in mitochondria, chloroplasts and bacteria, and is driven by proton gradient energy. The second occurs in bacteria when metabolic conditions dictate, generating a proton gradient to support nutrient uptake and locomotion. In the past, virtually all workers have assumed that the two reactions are reversible using the same reaction intermediates although, as we discuss, there are good arguments for writing separate, non-reversible schemes. The hydrolysis reaction has been studied in far greater depth and detail because of the availability of large amounts of soluble F_1 and because of its comparative ease of manipulation and experimental study. For ATP hydrolysis, we are now in a position to describe the mechanism of enzymatic rate acceleration in detail, and that is the purpose of this article. Work from our laboratory has utilized the *Escherichia coli* enzyme so that, strictly speaking, the statements made here refer to that system. However, given the extensive similarity between the F_1 portions of ATP synthases across species boundaries, we expect the conclusions to be of general applicability.

Catalytic sites of F_1

X-ray structure analyses (Abrahams et al., 1994, 1996; Van Raaij et al., 1996; Shirakihara et al., 1997; Orriss et al., 1998; Bianchet et al., 1998) show the three catalytic sites of F_1 at interfaces between the α and β subunits, with the large majority of protein-to-nucleotide ligands provided by the β subunit. The three sites appear structurally asymmetric when binding Mg–nucleotide, consistent with direct MgATP and MgTNPATP equilibrium binding studies (Weber et al., 1993, 1994b; Weber and Senior, 1996). The binding affinities for substrate MgATP are of the order of $1\,\mathrm{nmol\,l^{-1}}$, $1\,\mathrm{\mu mol\,l^{-1}}$ and $100\,\mathrm{\mu mol\,l^{-1}}$, respectively, at sites 1, 2 and 3, these values being the same in F_1 and in F_1F_0 (Weber et al., 1993; Löbau et al., 1998). Given the cellular concentrations of MgATP (e.g. $3\,\mathrm{mmol\,l^{-1}}$ in *E. coli*; Kashket, 1982; Mathews, 1972), it is evident that under physiological conditions all three catalytic sites will be filled and there will be no permanently unfilled or 'open' site (Löbau et al., 1997a).

In addition to three catalytic sites, F_1 contains three noncatalytic sites that bind MgATP but do not hydrolyze it. This provided a rich ground for confusion and controversy in past studies, since it was often uncertain to which sites added nucleotide was binding. However, the discovery of an engineered tryptophan probe which specifically monitors the occupancy of the noncatalytic sites (Weber et al., 1994a, 1995; Weber and Senior, 1995, 1997a) solved this problem, and it is now clear that the noncatalytic sites play no direct or regulatory role in hydrolysis. Indeed, the reaction proceeds at a normal rate whether the noncatalytic sites are filled or empty, confirming earlier work (Wise and Senior, 1985).

Filling of catalytic site 1 alone with MgATP yields an

extremely low net hydrolysis rate of approximately $0.001 \, \text{s}^{-1}$ (Penefsky and Cross, 1991), which is termed 'unisite catalysis'. Filling of two sites simultaneously ('bisite catalysis') yields substantial rate acceleration, up to a few per cent of the maximum rate, $V_{\max}$. However, to achieve physiological rates capable of sustaining cell viability (approximately $100 \, \text{s}^{-1}$), all three sites must fill with MgATP ('trisite or multisite catalysis') (Weber et al., 1993, 1999; Löbau et al., 1998). From the foregoing, it is apparent that, in addition to such usual factors as substrate binding energy and transition-state stabilization, which operate in single-site and non-cooperative enzymes, positive catalytic cooperativity between catalytic sites represents a major level of rate acceleration in F_1. This aspect of catalysis is not yet understood in molecular terms and represents a task for the future.

Under conditions of rapid, steady-state, multisite hydrolysis, two of the catalytic sites contain bound MgADP and the third contains bound MgATP (Weber et al., 1996). When F_1 is trapped in a catalytic transition state by use of the transition state analog MgADP•fluoroaluminate, all three catalytic sites are seen to be filled by nucleotide (Nadanaciva et al., 1999a). One site contains MgADP•fluoroaluminate bound with extremely high affinity, which represents a true transition-state complex. A second site contains MgADP•fluoroaluminate bound more weakly, possibly with partial transition-state-like structure, and the third site contains MgADP. At the time of writing, it seems likely that only site 1 actually carries out the hydrolysis reaction at any given time; however, this has not yet been proved.

Proposed mechanism of steady-state MgATP hydrolysis

Fig. 1 shows the mechanism that we currently favor to describe MgATP hydrolysis by F_1. Beginning at state D, the product MgADP has just dissociated, leaving one catalytic site empty (O). The other two sites are of high (H) and medium (M) affinity (sites 1 and 2 respectively). This corresponds to the state of the enzyme in the X-ray structure of Abrahams et al. (1994), with site O equivalent to the open 'βE' subunit. On binding of MgATP, site O closes fully or partially to give a site of low affinity (L) in state A. MgATP binding triggers a conformational event (call it number 1), which promotes rapid hydrolysis of MgATP at site H. We propose that the hydrolysis reaction *per se* causes another major conformational event (number 2), which brings about a change in binding affinity at each of the three sites (shown by arrows in state B). Finally inorganic phosphate (P_i) and MgADP dissociate (state C and back to state D).

The striking demonstration of ATP-driven rotation of the γ-subunit within the $\alpha_3\beta_3$ hexagon (Noji et al., 1997) provides a compelling argument for the idea that the three catalytic sites switch their identities and therefore affinities with each $120°$ arc of γ-rotation, and this concept of a 'binding change' has been incorporated into virtually all models of ATP hydrolysis. We speculate that, in the mechanism described in Fig. 1, the first conformational event, which occurs upon binding of
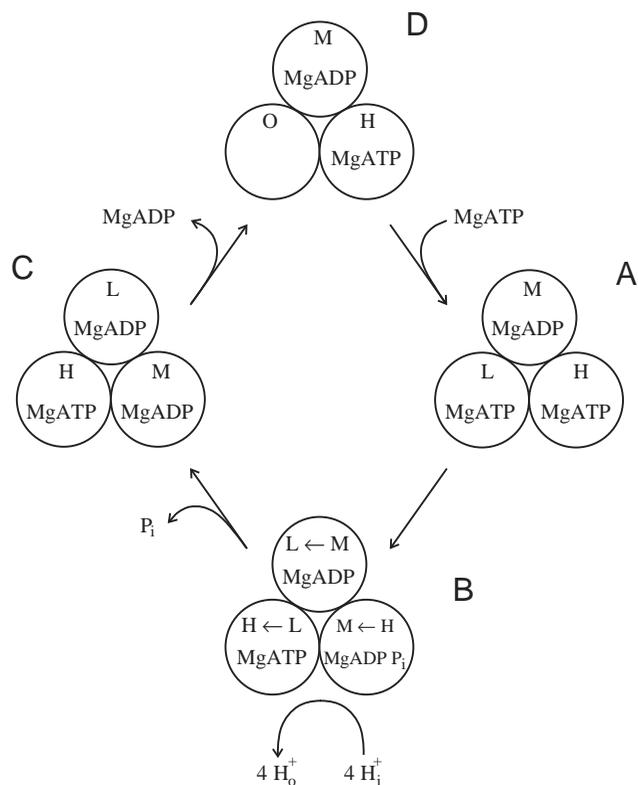

Fig. 1. Proposed mechanism for MgATP hydrolysis by F_1F_0-ATP synthase under steady-state, multisite conditions. In one complete cycle of MgATP hydrolysis, the enzyme passes through states A–D. The three catalytic sites are labelled H (site 1 of highest affinity), M (site 2 of intermediate affinity) and L (site 3 of lowest affinity). These are all occupied states, and the β subunit is closed. In state D, an open conformation of the catalytic site (O) occurs transiently, as product release from site L leaves this site temporarily empty. The mechanism is discussed in detail in the text. Note that the diagrammatic representation of the enzyme molecule is turned $120°$ anticlockwise at the C to D step.

MgATP, is caused by the βE (site O, open β subunit) closing fully or partially (state D to state A). This closing moves the γ subunit, perhaps by up to $60°$, to bring it in apposition with α subunits. Rapid hydrolysis of MgATP ensues at site 1 (H) (state A to state B), and the reaction moves first the α/β interface at site H and, as a consequence, also the γ subunit. The mechanical trigger for this second conformational event occurs at the α/β interface as the progression of the hydrolytic reaction first through a pentacovalent phosphorus transition state and then through a separation of MgADP from P_i drags residues across this interface. The γ subunit moves around to complete a $120°$ arc, thus causing the binding affinity change by making new contacts to the β subunits adjacent to the ones it originally contacted in state A. The β subunit that was originally site M has now become site L and is free to assume the open state, which spontaneously allows dissociation of product MgADP. Proton movement is linked to conformational event number 2, i.e. the same movement of γ that brings about the binding affinity change.

As to the question of whether ATP synthesis and hydrolysis are reversible using the same reaction intermediates, i.e. by simply utilizing bidirectional arrows in Fig. 1, we now believe there are good arguments for exploring separate, non-reversible schemes. First, it may be noted that whereas isolated F_1 and F_1F_o do not bind P_i to any extent at cellular (5 mmol l^{-1}) concentration in the absence of a proton gradient (Weber et al., 1993; Löbau et al., 1998), the K_m for P_i during ATP synthesis is approximately 1 mmol l^{-1} (Wise and Senior, 1985; Fischer et al., 1994; Al-Shawi et al., 1997). The presence of the proton gradient during ATP synthesis increases the affinity for P_i by orders of magnitude, in effect causing a phosphate binding pocket to form in the catalytic site where one did not previously exist. The proton gradient also modulates binding site affinity for MgATP to allow product release during ATP synthesis (Weber and Senior, 1997b; Al-Shawi et al., 1997). Second, ATP-induced rotation of the γ subunit is probably driven, at least in part, by the reaction step of hydrolysis, whereas in the synthesis direction, the rotation of the γ subunit is F_o-induced and drives affinity changes in the catalytic sites, with the reaction step thought to be spontaneous.

Derivation of Gibbs free energy diagrams and binding energies

In earlier work, our laboratory derived Gibbs free energy diagrams to describe the catalytic pathway of unisite MgATP hydrolysis in wild-type and several mutant enzymes (Al-Shawi et al., 1990; Senior and Al-Shawi, 1992). Difference energy diagrams for mutant *versus* wild type revealed steps that were differentially affected by mutations. Binding energies at each distinct catalytic step were deduced, from which it was apparent that there were two steps in the pathway at which major energetic transitions occurred, namely P_i binding/release and MgATP binding/release. The mutant enzymes used were ones then available and known to impair catalysis, but specific roles could not be assigned in the absence of structural information. However, it could be concluded that the catalytic site behaved in general as a catalytic surface in which multiple interactions between protein and MgATP were important and contributed incrementally to catalysis by providing binding energy in a sequestered and hydrophobic environment. Extension of this work to multisite hydrolysis through the use of Arrhenius plots and comparison of multisite *versus* unisite characteristics of mutant enzymes indicated that multisite catalysis, although clearly accelerated by additional factors, retained essential unisite interactions (Al-Shawi et al., 1990). Studies utilizing unisite catalysis must be viewed as empirical, since the experimental conditions are far from physiological. Because they avoid the complexities introduced by cooperative site–site interactions, however, they have served to simplify the system and have proved valuable for this reason.

After the X-ray structures became available, and with the discovery of specific engineered tryptophan probes to monitor catalytic site occupancy by Mg-nucleotides under steady-state, multisite hydrolysis conditions (Weber et al., 1993, 1996, 1998b), it has become possible to assign specific catalytic roles to catalytic site residues, as will be described in the next three sections.

### Mg^{2+} ligands confer catalytic site asymmetry and are essential for catalysis

Octahedral coordination of the Mg^{2+} in the MgATP substrate molecule is achieved by direct first-sphere liganding from O atoms of the β and γ phosphates and from the hydroxyl side-chain of residue β-Thr156 (the residue at the end of the Walker A consensus sequence), by second-sphere liganding through a water molecule hydrogen-bonded to the carboxyl of residue β-Asp242 (the residue at the end of the Walker B consensus sequence) and by second-sphere liganding to two water molecules hydrogen-bonded to the two oxygens of the carboxyl of residue β-Glu185 (Weber et al., 1998a). Fig. 2 shows the proposed arrangement of these ligands around the Mg^{2+}. Octahedral coordination is optimal at the site occupied by MgADP in the X-ray structure of Abrahams et al. (1994) (βDP), but somewhat distorted at the other occupied site (βTP), and on this basis we think these sites probably correspond to site 1 and site 2, respectively.

MgATP is the substrate, and there is no hydrolysis of free ATP. Removal of any one of the Mg^{2+} ligands by side-chain mutagenesis impairs hydrolysis very strongly (by 2–3 orders of magnitude). Free ATP binds to the three catalytic sites with equal and relatively weak affinity (approximately 100 μmol l^{-1}), in marked contrast to the asymmetry seen with MgATP described above (Weber et al., 1994b, 1998a). An X-ray structure of F_1 obtained at saturating ATP concentration in the absence of added Mg^{2+} shows the three catalytic sites filled with nucleotide, but in a largely symmetrical arrangement (Bianchet et al., 1998), in agreement with the binding data. A catalytic transition state is not achieved with ADP and fluoroaluminate in the absence of Mg^{2+} (Nadanaciva et al., 1999a). Thus, it is clear that the engagement of the Mg^{2+} ligands and the degree to which optimal octahedral coordination is achieved are critical factors in catalytic site substrate binding asymmetry and in catalysis. The γ subunit is distant from the catalytic sites and is unable to provide any direct ligands to the bound nucleotide; its contribution to catalytic site asymmetry must be indirect. By presenting three different faces, one to each of the β subunits, the γ subunit should be able to impose different conformational forms on each β subunit, leading to differential engagement of the Mg^{2+} ligands at the three catalytic sites.

Three positively charged residues stabilize the catalytic transition state

MgADP•fluoroaluminate binding was used as a probe of the catalytic transition state, and it was found that three positively charged residues located in the catalytic site, namely β-Lys155 (the 'Walker A Lys'), β-Arg182 and α-Arg376, are each required for transition-state stabilization (Nadanaciva et al.,

Fig. 2. Ligands to the Mg²⁺ of bound MgATP substrate in the F₁ catalytic site. The proposed octahedral coordination of Mg²⁺ (green) of MgATP. In the first coordination sphere are oxygens (large red spheres) from the β- and γ-phosphates of ATP and β-Thr156 hydroxyl. In the second coordination sphere are three waters (cyan) liganded to carboxyl oxygens of β-Asp242 and β-Glu185. Solid black lines show bonds. Dashed black lines are used to outline the octahedron formed by the Mg²⁺ ligands. The figure was created using Rasmol software, courtesy of Dr Roger Sayle, based on the X-ray structure of the βTP catalytic site of Abrahams et al. (1994). *Escherichia coli* residue numbering is used.
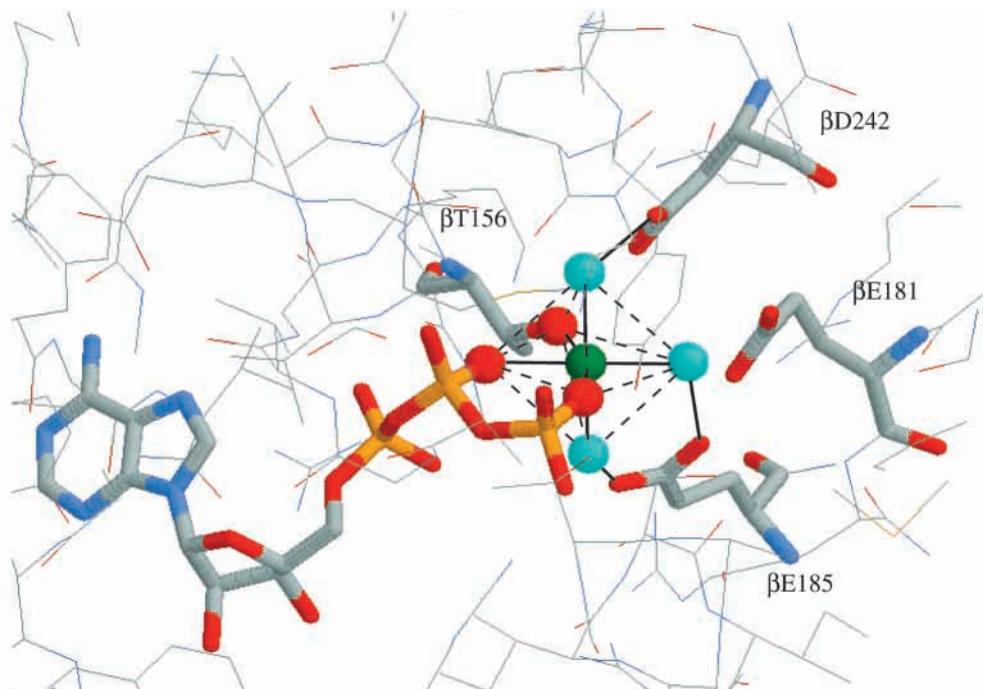
1999a,b; S. Nadanaciva and A. E. Senior, unpublished work). Mutagenesis of any one of these had a strong effect on catalysis, reducing ATPase activity by three or more orders of magnitude. These three residues are well-placed to hydrogen bond to a pentacovalent trigonal bipyramidal phosphorus transition state, as shown in Fig. 3. In addition, residues β-Lys155 and β-Arg182 also drive hydrolysis forward by providing substantial binding energy for MgATP through interaction with the γ-phosphate, especially at site 1 (Löbau et al., 1997b; Nadanaciva et al., 1999b), yet at the same time they do not stabilize binding of product MgADP to any significant extent. Interestingly, residue α-Arg376, despite its apparent proximity to the bound nucleotide in the X-ray structures,

appears to have little effect on MgATP or MgADP binding (S. Nadanaciva and A. E. Senior, unpublished work). This residue therefore shows certain parallels to the Arg residues from GTPase-activating proteins that activate catalysis in G-proteins by inserting into the catalytic site (Scheffzek et al., 1997; Rittinger et al., 1997). In F₁, catalysis will be possible only after assembly of α and β subunits into a complex, because only then will α-Arg376 be inserted into the catalytic site. This requirement provides an explanation for the fact that isolated β-subunit is hydrolytically inactive (Al-Shawi et al., 1991) and provides a neat regulatory device to prevent ATP hydrolysis by newly synthesized β subunit during assembly of F₁Fₒ in the cell.

Fig. 3. Proposed structure of the catalytic transition state in the F₁ catalytic site. A pentacovalent phosphorus transition state is shown. The Mg²⁺ is green, the putative attacking water is cyan. Solid black lines represent the apical bonds. Dashed black lines represent interactions that stabilize the transition state. The figure was created using Rasmol software, courtesy of Dr Roger Sayle, based on the X-ray structure of the βTP catalytic site of Abrahams et al. (1994). *Escherichia coli* residue numbering is used.
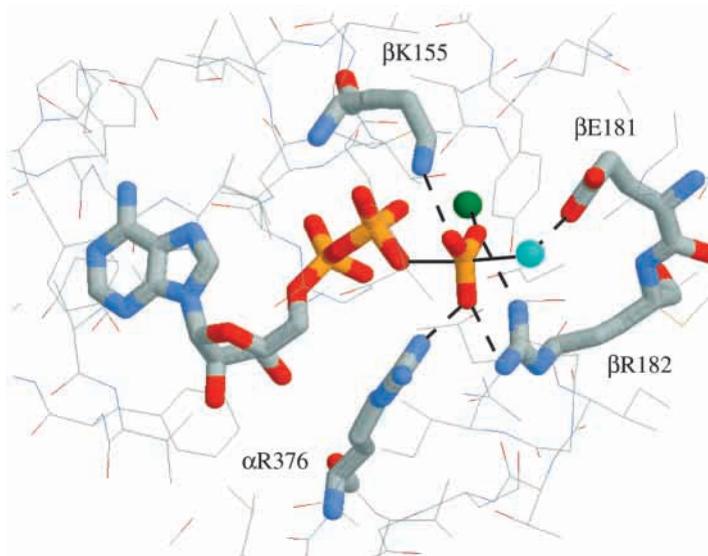
Residue β-Glu181 stabilizes the transition state and binds the attacking water

β-Glu181 appears to ligand through its carboxyl oxygens to a specific water molecule positioned appropriately to make nucleophilic attack at the γ-phosphorus (Abrahams et al., 1994). Whether base-catalysis is involved has been debated elsewhere (Weber and Senior, 1997b). Mutagenesis of β-Glu181 has very large impairing effects on catalysis (Senior and Al-Shawi, 1992; Park et al., 1994), reducing hydrolysis by three or more orders of magnitude, e.g. in the Gln mutant. Transition-state stabilization was abolished by mutagenesis of β-Glu181 to Gln (Nadanaciva et al., 1999a); however, no significant effects were seen on MgATP or MgADP binding (Löbau et al., 1997b) or Mg^{2+} liganding (Weber et al., 1998a). The unique role of β-Glu181 therefore appears to be to immobilize and polarize the attacking water, and the data provide good evidence for a substantially associative reaction mechanism. Fig. 3 shows the position of β-Glu181 in our representation of the likely transition-state structure, with the attacking water also shown.

Two mutations studied in earlier work and known to have large, deleterious effects on catalysis were β-Met209 to Ile and β-Arg246 to Cys (Al-Shawi et al., 1990). A ready explanation for the effects of these mutations is now apparent from the X-ray structures; both are in close proximity to residue β-Glu181. β-Met209 lies 0.3–0.4 nm away from β-Glu181 (depending on the exact atoms compared) and directs it towards the γ-phosphate of MgATP, consistent with our previous conclusion that mutagenesis of β-Met209 perturbs the environment of the catalytic site close to the site at which chemical bond cleavage occurs (Al-Shawi et al., 1990). β-Arg246 is even closer to β-Glu181, and a hydrogen bond is likely between the Arg NE nitrogen and one of the Glu carboxyl oxygens, at a distance of 0.29 nm. We suggested previously a role for β-Arg246 in conformational signal transmission necessary for multisite catalysis (Al-Shawi et al., 1990); in all probability, this role is linked to movement of β-Glu181. These mutations emphasize the need for strict stereochemisty in this region, consistent with the proposed role of β-Glu181.

Rate acceleration achieved by F₁Fₒ-ATP synthase

Non-enzymatic rates of MgATP hydrolysis at neutral pH in the literature are as follows: $10^{-5}\,s^{-1}$ at 80 °C (Tetas and Lowenstein, 1963), $2\times10^{-6}\,s^{-1}$ at 60 °C (Admiraal and Herschlag, 1995) and $5\times10^{-7}\,s^{-1}$ at 50 °C (Milburn et al., 1985). Thus, the value of $3.8\times10^{-9}\,s^{-1}$ at 23 °C quoted by Mildvan (1997) seems reasonable. At neutral pH and 23 °C, typical MgATP hydrolysis rates for different ATP synthases are $50–100\,s^{-1}$. The rate acceleration achieved by ATP synthase is therefore of the order 10^{11} (Mildvan, 1997, gives an estimate of $10^{10.7}$). It is apparent that, as Mildvan has already pointed out, the effects of mutations within the catalytic site are not additive. Considering β-Lys155, β-Arg182, α-Arg376 and β-Glu181 only, the sum of the impairment created by mutation of these residues

individually already exceeds the total catalytic capacity of the enzyme, and further contributions to rate acceleration from other residues, e.g. β-Tyr331, which are known to contact the substrate, would be expected. Thus, the catalytic effects of these residues are cooperative, as expected for the mechanisms proposed here.

Conclusions

Rate acceleration of ATP hydrolysis in ATP synthase is brought about by a number of factors. (1) Provision of substrate binding energy by residues lining the catalytic site. β-Lys155 and β-Arg182 are specific examples, both of which show differential binding of substrate MgATP *versus* product MgADP and also differential binding of MgATP at the three catalytic sites. (2) Liganding of Mg^{2+} in the Mg–nucleotide substrate, involving catalytic site side-chains from residues β-Thr156, β-Glu185 and β-Asp242. (3) Stabilization of the catalytic transition state by positively charged β-Lys155, β-Arg182 and α-Arg376. (4) Binding of the substrate water and stabilization of the transition state by the specific 'catalytic carboxylate' β-Glu181. (5) Positive catalytic cooperativity, induced by binding of MgATP to the second and third sites on the enzyme. The molecular basis of this last factor remains to be elucidated.

References

Abrahams, J. P., Buchanan, S. K., Van Raaij, M. J., Fearnley, I. M., Leslie, A. G. W. and Walker, J. E. (1996). The structure of bovine F₁-ATPase complexed with the antibiotic inhibitor efrapeptin. *Proc. Natl. Acad. Sci. USA* **93**, 9420–9424.

Abrahams, J. P., Leslie, A. G. W., Lutter, R. and Walker, J. E. (1994). Structure at 0.28 nm resolution of F₁-ATPase from bovine mitochondria. *Nature* **370**, 621–628.

Admiraal, S. J. and Herschlag, D. (1995). Mapping the transition state for ATP hydrolysis: implications for enzymatic catalysis. *Chem. Biol.* **2**, 729–739.

Al-Shawi, M. K., Ketchum, C. J. and Nakamoto, R. K. (1997). The *Escherichia coli* F₀F₁ γM23K uncoupling mutant has a higher $K_{0.5}$ for P_i. Transition state analysis of this mutant and others reveals that synthesis and hydrolysis utilize the same kinetic pathway. *Biochemistry* **36**, 12961–12969.

Al-Shawi, M. K., Parsonage, D. and Senior, A. E. (1990). Thermodynamic analyses of the catalytic pathway of F₁-ATPase from *Escherichia coli*. *J. Biol. Chem.* **265**, 4402–4410.

Al-Shawi, M. K., Parsonage, D. and Senior, A. E. (1991). Adenosine triphosphatase and nucleotide binding activity of isolated β-subunit preparations from *Escherichia coli* F₁Fₒ-ATP synthase. *J. Biol. Chem.* **265**, 5595–5601.

Bianchet, M. A., Hullihen, J., Pedersen, P. L. and Amzel, L. M. (1998). The 2.8 Å structure of rat liver F₁-ATPase: Configuration of a critical intermediate in ATP synthesis/hydrolysis. *Proc. Natl. Acad. Sci. USA* **95**, 11065–11070.

Fischer, S., Etzold, C., Turina, P., Deckers-Hebestreit, G., Altendorf, K. and Gräber, P. (1994). ATP synthesis catalyzed by

the ATP synthase of *Escherichia coli* reconstituted into liposomes. *Eur. J. Biochem.* **225**, 167–172.

Kashket, E. R. (1982). Stoichiometry of the H⁺-ATPase of growing and resting, aerobic *Escherichia coli. Biochemistry* **21**, 5534–5538.

Löbau, S., Weber, J. and Senior, A. E. (1997a). Nucleotide occupancy of F$_1$-ATPase under crystallization conditions. *FEBS Lett.* **404**, 15–18.

Löbau, S., Weber, J. and Senior, A. E. (1998). Catalytic site nucleotide binding and hydrolysis in F$_1$F$_o$-ATP synthase. *Biochemistry* **37**, 10846–10853.

Löbau, S., Weber, J., Wilke-Mounts, S. and Senior, A. E. (1997b). F$_1$-ATPase: Roles of three catalytic site residues. *J. Biol. Chem.* **272**, 3648–3656.

Mathews, C. K. (1972). Biochemistry of deoxyribonucleic acid defective amber mutants of bacteriophage T4. *J. Biol. Chem.* **247**, 7430–7438.

Milburn, R. M., Gautum-Basak, M., Tribolet, R. and Sigel, H. (1985). Comparison of the effectiveness of various metal ions on the promoted dephosphorylation of adenosine 5′-triphosphate (ATP) and uridine 5′-triphosphate (UTP). *J. Am. Chem. Soc.* **107**, 3315–3321.

Mildvan, A. S. (1997). Mechanisms of signalling and related enzymes. *Proteins* **29**, 401–416.

Nadanaciva, S., Weber, J. and Senior, A. E. (1999a). Binding of the transition state analog MgADP-fluoroaluminate to F$_1$-ATPase. *J. Biol. Chem.* **274**, 7052–7058.

Nadanaciva, S., Weber, J. and Senior, A. E. (1999b). The role of β-Arg-182, an essential catalytic site residue in *Escherichia coli* F$_1$-ATPase. *Biochemistry* **38**, 7670–7677.

Noji, H., Yasuda, R., Yoshida, M. and Kinosita, K., Jr (1997). Direct observation of the rotation of F$_1$-ATPase. *Nature* **386**, 299–302.

Orriss, G. L., Leslie, A. G. W., Braig, K. and Walker, J. E. (1998). Bovine F$_1$-ATPase covalently inhibited with 4-chloro-7-nitrobenzofurazan: the structure provides further support for a rotary catalytic mechanism. *Structure* **6**, 831–837.

Park, M. Y., Omote, H., Maeda, M. and Futai, M. (1994). Conserved Glu-181 and Arg-182 residues of *Escherichia coli* H⁺-ATPase (ATP synthase) β subunit are essential for catalysis: Properties of 33 mutants between βGlu-161 and βLys-201 residues. *J. Biochem.* **116**, 1139–1145.

Penefsky, H. S. and Cross, R. L. (1991). Structure and mechanism of F$_o$F$_1$-type ATP synthases and ATPases. *Adv. Enzymol.* **64**, 173–214.

Rittinger, K., Walker, P. A., Eccleston, J. F., Smerdon, S. J. and Gamblin, S. J. (1997). Structure at 1.65 Å resolution of RhoA and its GTPase-activating protein in complex with a transition-state analog. *Nature* **389**, 758–762.

Scheffzek, K., Ahmadian, M. R., Kabsch, W., Wiesmüller, L., Lautwein, A., Schmitz, F. and Wittinghofer, A. (1997). The Ras–RasGAP complex: Structural basis for GTPase activation and its loss in oncogenic ras mutants. *Science* **277**, 333–338.

Senior, A. E. and Al-Shawi, M. K. (1992). Further examination of seventeen mutations in *Escherichia coli* F$_1$-ATPase β-subunit. *J. Biol. Chem.* **267**, 21471–21478.

Shirakihara, Y., Leslie, A. G. W., Abrahams, J. P., Walker, J. E.,

Ueda, T., Sekimoto, Y., Kambara, M., Saika, K., Kagawa, Y. and Yoshida, M. (1997). The crystal structure of the nucleotide-free α$_3$β$_3$ subcomplex of F$_1$-ATPase from the thermophilic *Bacillus* PS3 is a symmetric trimer. *Structure* **5**, 825–836.

Tetas, M. and Lowenstein, J. M. (1963). The effect of bivalent metal ions on the hydrolysis of adenosine di- and tri-phosphate. *Biochemistry* **2**, 350–357.

Van Raaij, M. J., Abrahams, J. P., Leslie, A. G. W. and Walker, J. E. (1996). The structure of bovine F$_1$-ATPase complexed with the antibiotic inhibitor aurovertin B. *Proc. Natl. Acad. Sci. USA* **93**, 6913–6917.

Weber, J., Bowman, C. and Senior, A. E. (1996). Specific tryptophan substitution in catalytic sites of *Escherichia coli* F$_1$-ATPase allows differentiation between bound substrate ATP and product ADP in steady-state catalysis. *J. Biol. Chem.* **271**, 18711–18718.

Weber, J., Bowman, C., Wilke-Mounts, S. and Senior, A. E. (1995). α-Aspartate 261 is a key residue in noncatalytic sites of *Escherichia coli* F$_1$-ATPase. *J. Biol. Chem.* **270**, 21045–21049.

Weber, J., Dunn, S. D, and Senior, A. E. (1999). Effect of ε-subunit on nucleotide binding to *Escherichia coli* F$_1$-ATPase catalytic sites. *J. Biol. Chem.* **274**, 19124–19128.

Weber, J., Hammond, S. T., Wilke-Mounts, S. and Senior, A. E. (1998a). Mg^{2+} coordination in catalytic sites of F$_1$-ATPase. *Biochemistry* **37**, 608–614.

Weber, J. and Senior, A. E. (1995). Location and properties of pyrophosphate binding sites in *Escherichia coli* F$_1$-ATPase. *J. Biol. Chem.* **270**, 12653–12658.

Weber, J. and Senior, A. E. (1996). Binding and hydrolysis of TNP-ATP by *Escherichia coli* F$_1$-ATPase. *J. Biol. Chem.* **271**, 3474–3477.

Weber, J. and Senior, A. E. (1997a). Binding of TNP-ATP and TNP-ADP to the noncatalytic sites of *Escherichia coli* F$_1$-ATPase. *FEBS Lett.* **412**, 169–172.

Weber, J. and Senior, A. E. (1997b). Catalytic mechanism of F$_1$-ATPase. *Biochim. Biophys. Acta* **1319**, 19–58.

Weber, J., Wilke-Mounts, S., Grell, E. and Senior, A. E. (1994a). Tryptophan fluorescence provides a direct probe of nucleotide binding in the noncatalytic sites of *Escherichia coli* F$_1$-ATPase. *J. Biol. Chem.* **269**, 11261–11268.

Weber, J., Wilke-Mounts, S., Hammond, S. T. and Senior, A. E. (1998b). Tryptophan substitutions surrounding the nucleotide in catalytic sites of F$_1$-ATPase. *Biochemistry* **37**, 12042–12050.

Weber, J., Wilke-Mounts, S., Lee, R. S. F., Grell, E. and Senior, A. E. (1993). Specific placement of tryptophan in the catalytic sites of *Escherichia coli* F$_1$-ATPase provides a direct probe of nucleotide binding: Maximal ATP hydrolysis occurs with three sites occupied. *J. Biol. Chem.* **268**, 20126–20133.

Weber, J., Wilke-Mounts, S. and Senior, A. E. (1994b). Cooperativity and stoichiometry of substrate binding to the catalytic sites of *Escherichia coli* F$_1$-ATPase. *J. Biol. Chem.* **269**, 20462–20467.

Wise, J. G. and Senior, A. E. (1985). Catalytic properties of the *Escherichia coli* proton adenosine triphosphatase: Evidence that nucleotide bound at noncatalytic sites is not involved in regulation of oxidative phosphorylation. *Biochemistry* **24**, 6949–6954.